Calcium Chemistry in the Microbial World

Stephanie Hanhan

4G06 Senior Thesis

Supervisor: Prof. Adam P. Hitchcock

McMaster University April 2007

Abstract: The artificial enhancement of bacterial induced calcite formation has been proposed to counter the adverse effects of fossil fuel combustion. This method of carbon dioxide sequestration necessitates an improved understanding of calcite biomineralization. Synchrotron based Scanning Transmission X-ray Microscopy (STXM) was used at the Canadian Light Source (CLS) and Advanced Light Source (ALS). Various calcium carbonate polymorphs and other calcium salts were studied at the calcium edge, in addition to investigating forms of calcium in the regions of calcite biomineralization. Ca 2p X-ray absorption spectroscopy was shown to differentiate calcite, aragonite and other calcium species. When applied to a biofilm sample, Ca 2p based chemically specific imaging was used to show a systematic development from Ca^{2+} associated with extra-cellular polysaccharides, through an aragonite-like intermediate, to the formation of calcite crystals. A better understanding of Ca 2p spectroscopy has shown that STXM can be used to identify an unknown form of calcium in a dry or biological sample. Using reference spectra from the Ca 2p edge, the stage is now set for systematic studies of calcite biomineralization in bacterial biofilms and in other biological samples.

Introduction

The delicate balance of life on Earth is sustained by the cycles that work to stabilize the environment. As a result of man's excessive fossil fuel combustion there has been a dramatic increase in atmospheric levels of carbon dioxide (CO_2). Prior to the industrial revolution (late 1800's), the global concentration of CO_2 in the atmosphere was about 280 parts per million by volume (ppmv) while the present concentration is about 370ppmv.[1] As atmospheric levels continue to increase and concern over climate change mounts, slowing the rate of increase of CO_2 in the atmosphere is of urgent interest.[2] CO_2 dissolution into large bodies of water, consumption via plant photosynthesis and carbon sequestration by underground storage in oil fields have all been suggested. Another promising idea is the precipitation of calcite. This has advantages over the aforementioned methods, namely its permanency. Presently, it is widely accepted that calcite formation is bacteria mediated, however the preliminary and intermediate stages have yet to be defined.[3] Since the long-term goal is the artificial enhancement of calcite formation to decrease atmospheric levels of CO_2, achieving a better understanding of the mechanism of biomineralization may assist rationale design of carbon sequestration schemes involving calcite formation.

To introduce, using an example, the obstacles involved in this investigation, a biofilm sample collected from Lake Lucerne will be discussed. Lake Lucerne, located in Switzerland, contains a thermocline. The thermocline is a layer of water between the surface layer and deep water layer over which there is a steep drop in temperature relative to its depth.[4] It is along this temperature boundary that one species of bacteria grows

wildly and calcite crystals are found. In order to investigate how the two are related, a biofilm sample was collected and analyzed by Dr. Martin Obst using Scanning

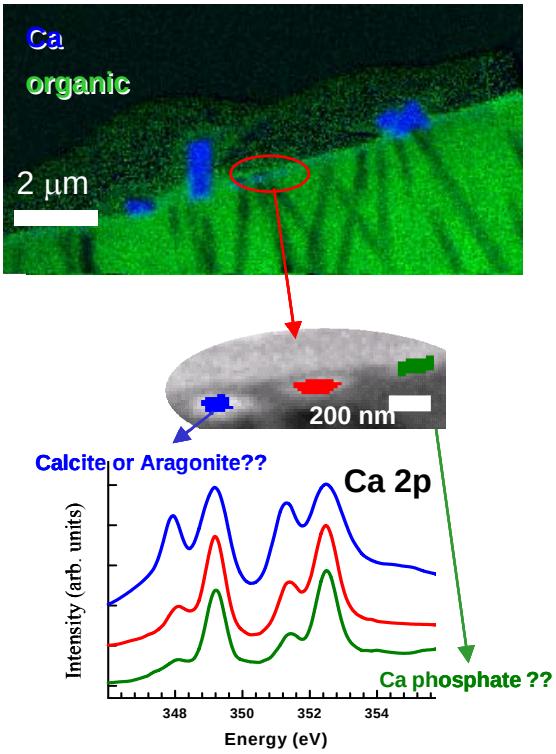

Transmission X-ray Microscopy (STXM) at the Advanced Light Source (ALS). As seen in Figure 1, large calcite crystals in blue and filamentous bacteria (dark green) within an epoxy (light green) are identified. By extracting spectra from smaller crystals closer to the bacteria and thus to the nucleation event, it is seen that three different calcium 2p spectra are observed. Understanding the relationship between the Ca 2p spectra and Ca^{2+} environment and thus helping to interpret the changing Ca environment in this bacterial biomineralization event, is the subject of this thesis.

Figure 1 – *Above:* An image of a thin biofilm section made by focus ion beam machining an epoxy embedded sample of bacteria collected in the thermocline region of Lake Lucerne. *Middle:* An image of three regions of nanometre scale crystals. *Bottom:* Different colour-coded spectra extracted from the three regions. (Martin Obst (McMaster), (STXM data recorded 14-Aug-06 at ALS STXM532)

My focus in this thesis is the use of Near Edge X-ray Absorption Fine Structure (NEXAFS) spectroscopy to probe the calcium 2p edge of various calcium compounds. Acquiring reliable spectra and better understanding them will help identify different forms of calcium in an unknown sample. This is exemplified in the classification of three calcium components in a dry biofilm sample, prepared by Dr. Obst at the CLS. In order to aid in the analysis of samples in solution or of biological origin, I designed a wet cell in which a wet environment can be created and maintained. Reliable Ca 2p reference spectra combined with the ability to analyze samples in solution will add a valuable piece to the puzzle that is the mechanism of biomineralization.

Methods

Near Edge X-ray Absorption Fine Structure (NEXAFS) Spectroscopy

In NEXAFS a soft X-ray is absorbed by the core level of an atom. NEXAFS is element specific since core levels of atoms occur at well defined energies. It provides information about the chemical environment of the core excited atom by the way the unoccupied energy levels combine with the symmetry of the core level to yield unique spectral features. A tunable source of soft X-rays is needed. Accordingly, NEXAFS is performed using synchrotron radiation. Synchrotron radiation is electromagnetic radiation emitted as electrons are accelerated.[5] While electrons are stored in a closed ring under ultrahigh vacuum, synchrotron radiation is emitted tangentially to the orbit. The natural polarization of synchrotron radiation is the reason that NEXAFS is sensitive to molecular orientation, where the σ or π bonds in an oriented, anisotropic crystalline solid are distinguishable.

Scanning Transmission X-ray Microscopy (STXM)

Soft X-ray spectromicroscopy was measured using STXM at the Canadian Light Source (CLS) in Saskatoon, Saskatchewan and at the ALS at the Lawrence Berkeley National Laboratory, Berkeley. Using mirrors, a grating monochromator and a zone plate, the beam is focused into the sample plane, the sample is then scanned and an X-ray detector counts transmitted X-rays. In STXM, focusing is done using a Fresnel zone plate which consists of alternating concentric rings of absorbing and transmitting material (opaque and transparent regions) such that the light deflected by the various zones converge at the focal point in phase.[6] STXM is a suitable technique for imaging biological and inorganic samples since it has a spatial resolution of approximately 50 nm. While the resolution is not as good as that in Transmission Electron Microscopy (TEM) the radiation damage suffered by the sample is three orders of magnitude less.[7] Another feature of STXM is that quantitative information is obtained since the transmitted intensity can be converted to optical density using Beer's law. Finally, since STXM is an X-ray in, X-ray out technique and soft X-rays penetrate water except at the O 1s edge, wet samples can be measured.

This research will focus in detail on the Ca 2p spectrum (345-356eV). The goal is to extract reliable Ca 2p spectra of known calcium compounds by rejecting those distorted by absorption saturation. This will help in the identification of the form of calcium in an unknown sample, as shown in the last section of this thesis. Furthermore, the ability of soft X-rays to penetrate water will be exploited when samples in solution are studied. Combining the specificity of NEXAFS with the resolution of STXM means that it is

possible to map a biological sample in terms of components of interest such as calcite, protein and polysaccharide. Spectra can be extracted from specific regions and compared with previously collected Ca 2p spectra in order to identify the form of calcium present. More reliable spectroscopy has lead to interesting preliminary results. However, more work is needed to fully contribute to understanding the mechanism of calcite biomineralization.

Wet Cell Design

In science, there is a great deal of value placed on studying systems that mimic or resemble actual systems of interest. When biomineralization is considered, analyzing dry samples of thin biofilms is useful, but cannot compare to examining a sample that is fully hydrated and alive. For this reason, one focus of this research is the development of a wet cell; a way to create and maintain a wet environment during data collection. While dry samples are mounted on a 3mm TEM grid or a silicon nitride window (Si_3N_4) in a silicon frame, wet samples are typically sandwiched between two of these windows. The Si_3N_4 windows are a 1mm x 1mm section in the centre of a 5mm x 5mm Si frame. The windows resemble a basket in that one side is flat while the other has a rut in it. To avoid creating a liquid layer too thick for X-rays to penetrate, the sample is sandwiched between the flat surfaces of the two windows. With this approach, the biggest obstacle is sealing the windows together before the few microlitres of sample inside evaporate. Previously, there was a high rate of failure of constructing cells even though various assemblies had been explored. As part of this thesis it was requested to design, fabricate and commission a reliable STXM wet cell. In doing so, I started with a liquid cell design

for STXM recently published by Stollberg et al, but made some significant improvements. The new wet cell features a two piece stainless steel design (exact

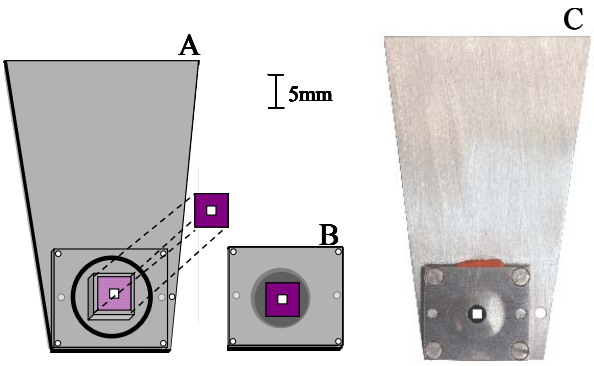

dimensions shown in Appendix A).[8] Shown in Figure 2, the bottom piece fits perfectly into gripping clasps inside the STXM, and supports the bottom window on a pedestal. In the pedestal, a groove has been made such that the window sits flush with the rim of the groove. The top piece has a circular depression in which a machined jig is used to centre the window. The most successful assembly is now described.

Figure 2 – A,B: Schematic of the wet cell, Si_3N_4 windows shown in purple Si frames. A: The window on the bottom piece is projected onto the pedestal where it rests; B: The top window in place on the top piece. C: Photograph of assembled wet cell, window emphasized in white to show position.

The bottom window is placed on the pedestal with the flat side of the window facing up, and all four edges are sealed to the steel base using 5-minute Epoxy™. Using the machined jig, the top window (flat side facing up) is centred and glued to the top piece using the same adhesive. After the glue on both pieces has dried completely, the rubber o-ring is lubricated with silicone grease and placed into its groove on the bottom part of the apparatus. Using a needle containing sample solution a few drops are placed onto the bottom or top window. Using pins to align the two pieces, the two windows are brought together and excess solution squeezes out. Screws in the corners are tightened uniformly

until interference fringes are observed in the windows, under an optical microscope. Holes located in the top and bottom edge of the top piece can be used to introduce sample solution into the plenum (the area surrounding the windows) using a 25-gauge needle; the holes are filled with Plasticine™. The wet cell not only seals each window to its support, but also seals the surrounding area via an o-ring. The two needle holes are filled with Plasticine™ to restrict air access that would dry out the sample.

Samples

The wet cell is used to study solutions while dry samples are prepared by dusting a crushed powder onto a Si_3N_4 window. $CaCl_2 \cdot 2H_2O$ is dissolved in deionized water to prepare a 0.5M solution while other samples – calcite, aragonite, $CaNO_3 \cdot 4H_2O$, $CaSO_4 \cdot 2H_2O$ – were recorded in the dry state. The source of the samples as well as the file references of collected data is found in Appendix B.

Results and Discussion

Ca 2p Spectroscopy

Inner shell spectroscopy is a very powerful analytical technique. However, using transmission measurements is complicated by a phenomenon known as absorption saturation, which occurs when the path length of a sample is too high and the soft X-rays are not transmitted. Absorption saturation is an energy dependent spectral distortion that occurs when samples are too thick.[9] Figure 3 is a cartoon representation of this phenomenon. Incoming soft X-rays of both first and second order are incident on the sample, shown in green. The grayscale box inside the sample represents X-rays as they

pass through the sample, while the corresponding spectra of detected transmission and OD are shown. The wings of the first order spectrum and second order spectrum are detected, but there is a difference in the transmission of X-rays when comparing energies on and off the resonance. Notice that at the peak there are no X-rays transmitted as a consequence of sample thickness. The resulting OD spectrum in turn is distorted, as the

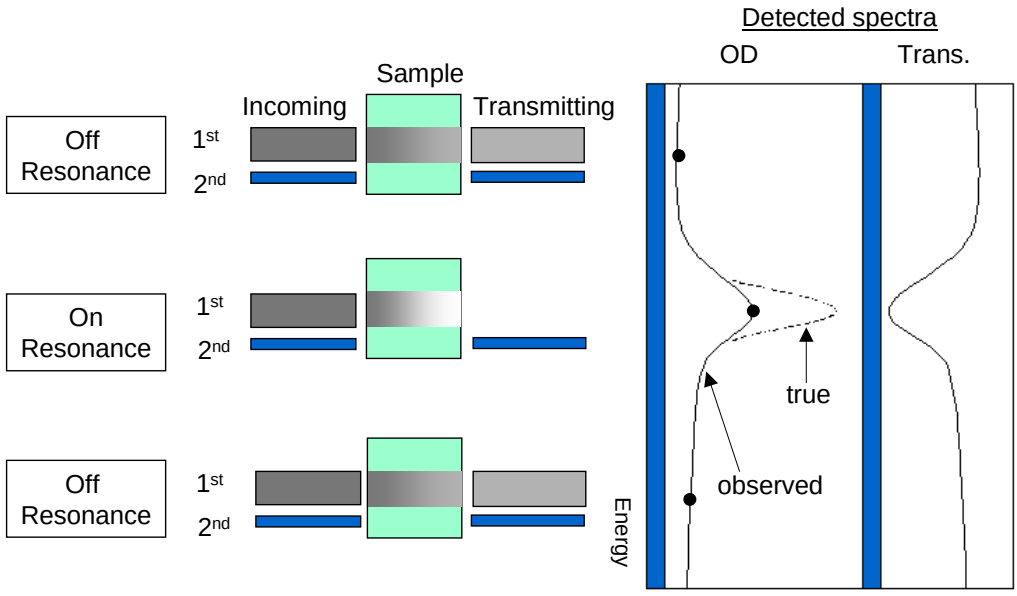

true peak is in fact not the same as the observed peak of decreased intensity. Accordingly, this phenomenon is particularly common when there are sharp, intense transitions as in the Ca 2p spectra. To avoid saturated spectra, it is necessary to optimize the sample thickness and to use as highly monochromated light as possible.

Figure 3 – Cartoon showing incoming and transmitting soft X-rays and resulting spectral distortion on resonance, in a sample undergoing absorption saturation.

In September 2006, STXM532 at the ALS was used to obtain an image of a calcium oxalate deposit by collecting a series of images at photon energies between 344-355eV. Subsequently, the images were converted to optical density using the area absent of sample as the I_0 region. By averaging the OD maps, Figure 4 was acquired. Next, the

program aXis 2000 was used to select specific values of OD as seen in the 3D display in Figure 5. Selecting optical density greater than 0.05OD selects the entire sample (less the background), whereas optical density greater than 0.2OD selects the majority of the sample, excluding the thinnest region at the edge of the crystal. By subtracting the two optical density maps, the red ring (Figure 5B) is what remains. In repeating this procedure by choosing increasing values of OD then subtracting the next closest value, each ring is isolated. Spectra from each of the annuli were then extracted and displayed in Figure 6.

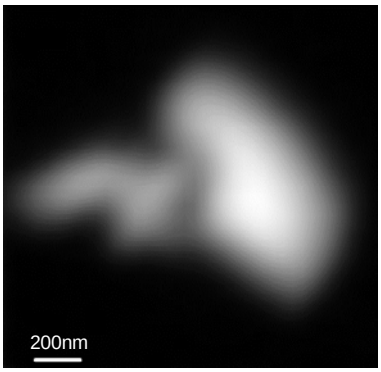

Figure 4 – OD mapping of a crystal of calcium oxalate (ALS STXM 532).

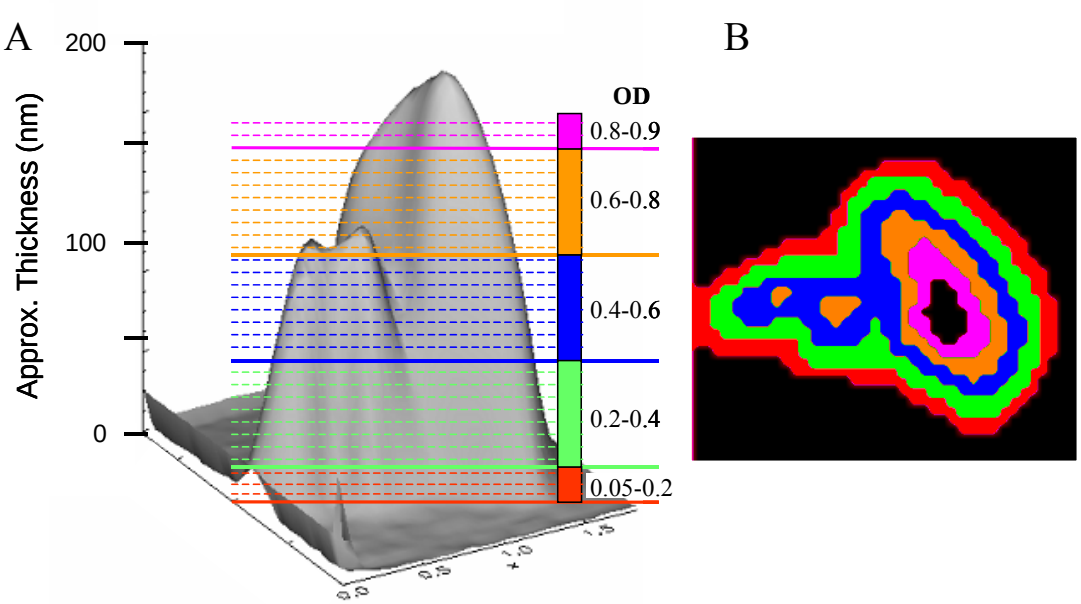

Figure 5 – A: 3D mapping of calcium oxalate crystal. Coloured regions are selected at specific OD to generate OD mask (B).

Figure 6A plots the spectra with offsets while Figure 6B plots with rescaling which more clearly shows the effect of absorption saturation. The Ca 2p spectrum of calcium oxalate has two main peaks and a complex structure at the leading edge of each peak. For the purpose of this explanation, only the two peaks at higher energy will be considered. When the spectra are stacked independently for shape comparison, it appears as though the intensity of the larger peak is decreasing relative to the smaller peak. This is more apparent in the rescaled plot (Figure 6B) which overlays the spectra showing that the spectra taken from regions of 0.6-0.8OD and 0.8-0.9OD are saturated whereas the distortion is not evident in the three spectra taken from lower OD regions. Referring to the 3D map in Figure 5 it appears that ~0.5OD is the upper limit for reliable Ca 2p spectra. This corresponds to a sample thickness of about 50 nm.

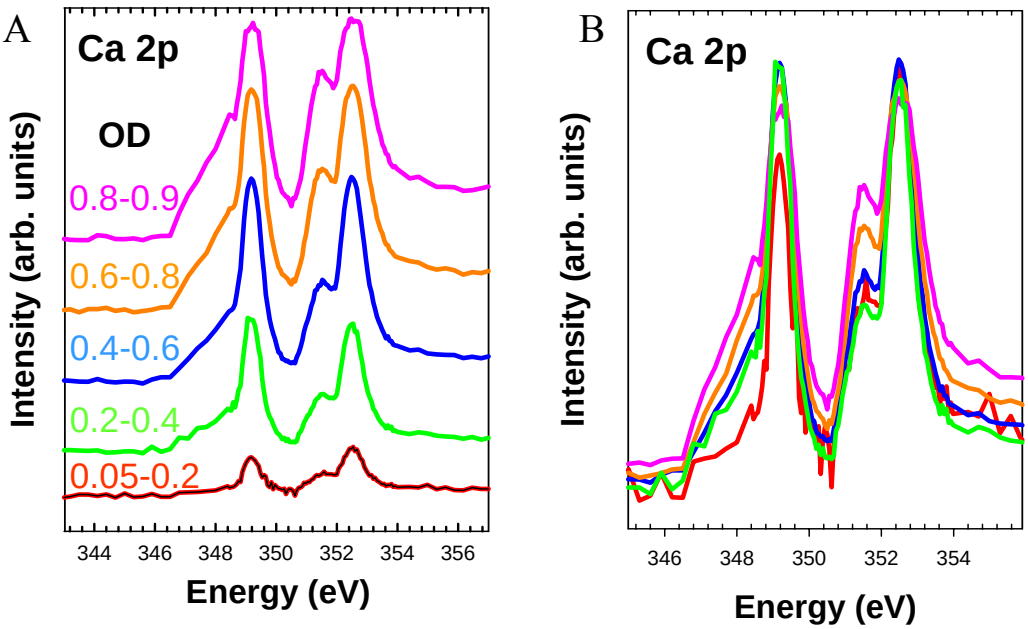

Figure 6 – A: Ca 2p spectra of Calcium oxalate in specific OD ranges stacked for shape comparison. B: Rescaled plot of spectra overlaid to show change indicative of absorption saturation (ALS STXM532).

The technique of examining spectra as a function of thickness by extracting annuli at increasing ranges of OD was applied to image sequences from small crystals of calcite and aragonite. Figure 7A shows the mask generated for a crystal of calcite and Figure 7B plots the extracted spectra. When compared to the spectra of calcium oxalate, these spectra do not show a decrease in intensity of the larger peak relative to the adjacent peak at lower energy.

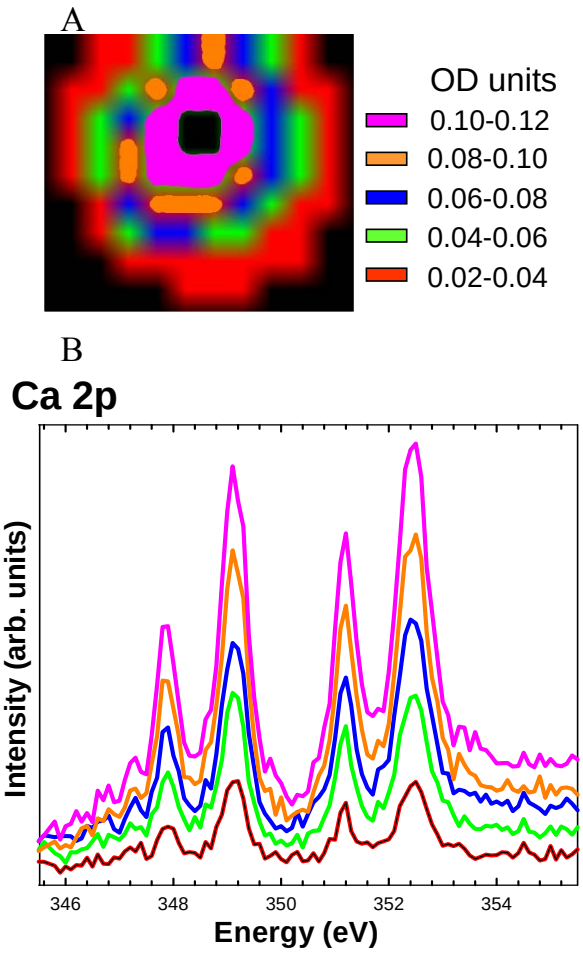

Figure 7 – A: OD map of a calcite crystal. B: Spectra colour coded according to region of crystal it represents (STXM CLS).

To mimic the previous comparison, the spectra are rescaled and over plotted. It is obvious from Figure 7B that both higher energy peaks are close enough to the same point

that it is justified to assume that no absorption saturation is occurring. In observing the values of OD, this should come as no surprise. The sample of calcium oxalate avoided absorption saturation only when the sample thickness had an optical density lower than 0.6OD. In this crystal of calcite however, the sample has 0.10-0.12OD at the thickest

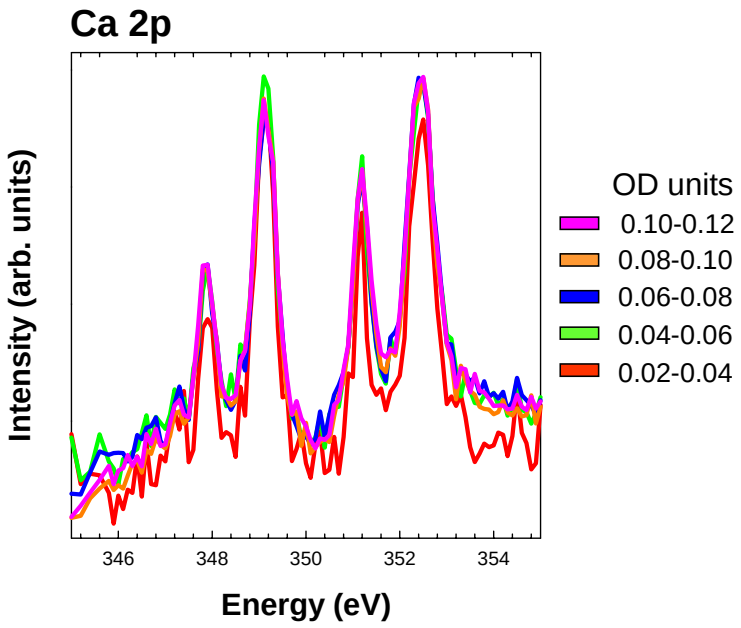

region, thus it is not expected to undergo saturation.

Figure 7B – Calcite spectra rescaled and overlayed for comparison (STXM CLS).

On the other hand, an image sequence from a sample of aragonite was analyzed, and

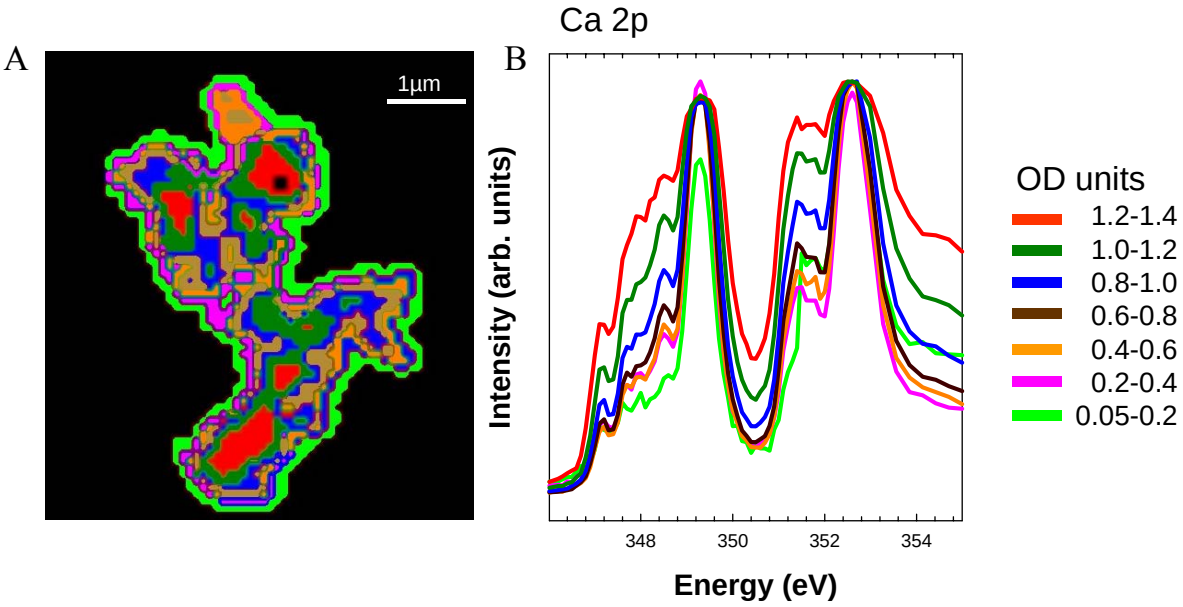

showed clear indications of absorption saturation. Figure 8A shows the generated OD masks; Figure 8B shows the extracted spectra. In Figure 8B, absorption saturation is apparent in the three thickest regions of the sample; those at 0.8OD and greater.

Figure 8 – A: OD map of a crystal of aragonite, B: Spectra extracted from aragonite sample (STXM CLS).

In selective data extraction from samples of calcium oxalate, calcite and aragonite, it is found that the thickest region from which data did not show spectral distortion are those with an optical density less than 0.6OD. After analysis of different salts of calcium a better understanding of Ca 2p spectra is achieved, making the exclusion of distorted spectra easier.

Spectral Shape

Figure 9, plots spectra of $CaCl_2 \cdot 2H_2O$, $CaNO_3 \cdot 4H_2O$, $CaSO_4 \cdot 2H_2O$, and $CaCO_3$ (calcite and aragonite), all taken from extremely thin regions of sample and thus considered reliable. This plot shows that the species of calcium is identifiable from its Ca 2p spectrum. It is interesting to examine the origin of these spectral differences.

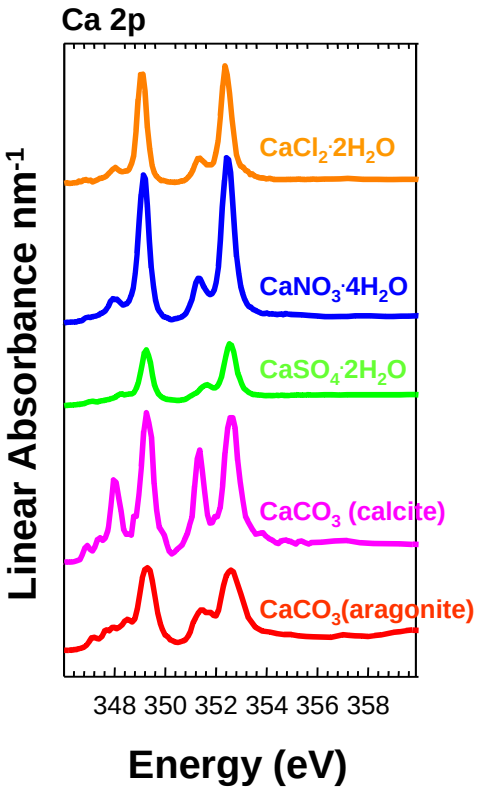

Figure 9 – Spectral shape comparison of various calcium salts ($CaCl_2 \cdot 2H_2O$, $CaNO_3 \cdot 4H_2O$, $CaSO_4 \cdot 2H_2O$, STXM532 ALS; calcite and aragonite, STXM CLS).

The electronic transition in calcium is the 2p→3d transition. The ground state electron configuration is $[Ne]3s^23p^6$ for Ca^{2+}, and the excited configuration is $[Ne]3s^23p^53d^1$. The $2p^63d^0 \rightarrow 2p^53d^1$ transition has three Pauli allowed multiplet states in an LS coupling picture: ^3F, ^3P and ^1D. This is one origin of the fine structure. A second is spin-orbit splitting of the 2p core hole. In a j-j coupling picture this yields $2p_{3/2}$ and $2p_{1/2}$ levels. Spectra are also determined by the crystal field and thus the calcium environment is relevant. While crystal field theory provides much of the explanation of 2p spectra, there will also be contributions from the extended orbital character of the molecular anions and thus ligand field theory should be used.[11] Figure 10 shows calculated and experimental spectra of octahedral, 6-coordinate calcium oxide (CaO) and cubic, 8-coordinate fluorite (CaF_2).[12] There are four main peaks generated by spin-orbit splitting and the crystal field, assigned $2p_{3/2}$-t_{2g}, $2p_{3/2}$-e_g, $2p_{1/2}$-t_{2g}, $2p_{1/2}$-e_g with increasing energy.[12] In both spectra, the weak peaks are attributed to a mixing of states from the interaction between the core hole and the valence electron combined with 3d spin-orbit splitting.[12] Both spectra have four peaks as expected however they are clearly different. In CaO, calcium is in a 6-coordinate octahedral environment whereas in fluorite calcium is 8-coordinate. The consequence of cubic coordination is that the order of the t_{2g} and e_g orbitals reverse and the intensity of the peaks from the e_g orbitals drops.[12] In neither case are the spectra simple to assign. For example the more intense $2p_{3/2}$ peaks cannot be easily assigned even though the e_g peaks have decreased intensity. Suffice it to say that the complexity of the spectra is a result of multiple effects. Furthermore, the line shape for each line is determined by both Gaussian and Lorentzian broadening mechanisms. Detailed

computational study of the Ca 2p spectra reported in this thesis is beyond the scope of the project but is a suitable goal for following studies.

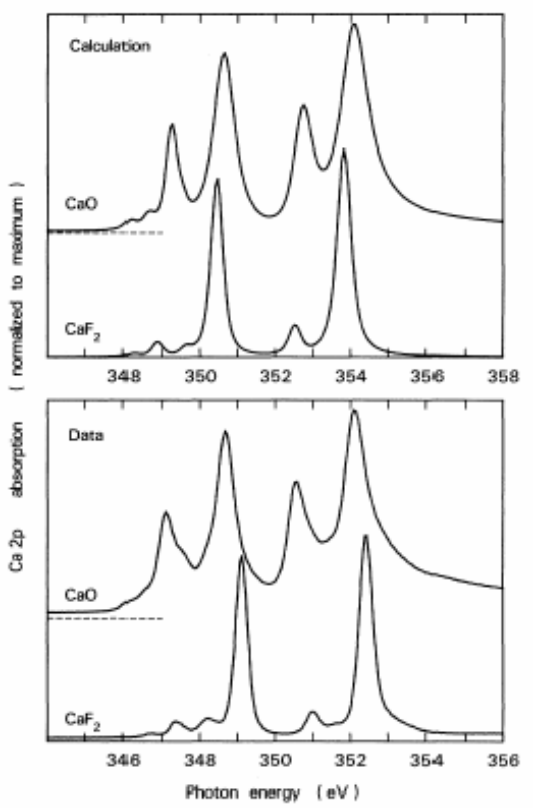

Figure 10 – Calculated and experimental Ca 2p spectra for Ca^{2+} in CaO and CaF_2.[12]

Hanhan™ Wet cell

The goal of understanding the mechanism of calcite formation in bacterial biofilms is aided by the formation of a database of trustworthy Ca 2p spectra. However most biofilm samples studied previously were dry. The purpose of developing a wet cell was to provide a reliable sample holder to measure the spectrum from calcium ions in solution and from biological samples. Using the stainless steel wet cell designed and machined at McMaster University, a sample of deionized water was introduced between two 100nm thick Si_3N_4 windows and tested for leaks. Figure 11 shows the O 1s spectrum collected from this cell using STXM (CLS), compared with a reference spectrum of water collected

previously at the ALS. This data confirms that after making a wet sample, the cell seals and a water spectrum can be obtained even while the wet cell is in a bone dry 1/3rd atmosphere of helium in the STXM.

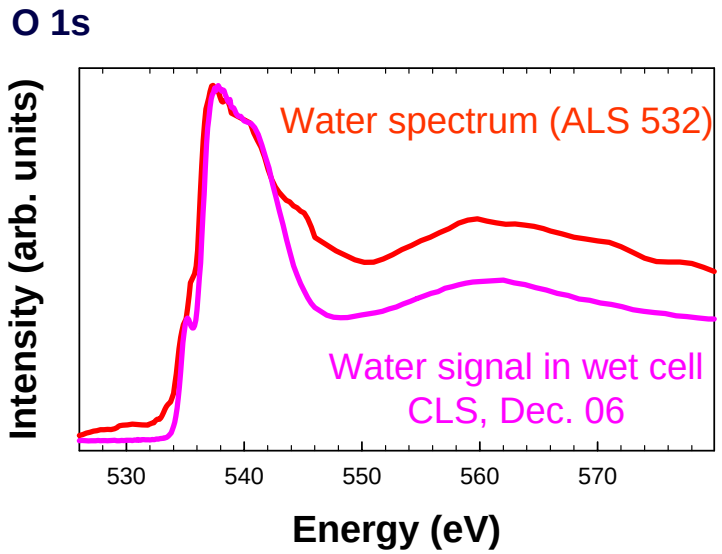

Figure 11 – Reference water spectrum collected at the ALS (red) compared with the O1s signal from the Hanhan^{TM} wet cell (purple)(CLS).

When dry samples are analyzed, the optical density is used to extract sample thickness. Samples in solution differ in that there is a very thick water layer (relative to the sample thickness) in addition to the ion of interest. Consequently, the solution concentration must be adjusted to avoid masking the ionic signal by that of the water. Consider the region between the two silicon nitride windows to be a column of water ~2000nm thick. Looking at the Ca 2p edge, a sample thickness of ~50nm is desired. 50nm of Ca^{2+} in 1950nm of solution corresponds to a desired solution concentration of 0.5M. In order to attain such a high concentration it is essential that a highly soluble salt be used hence the very soluble $CaCl_2{\cdot}2H_2O$ was selected and a 0.5M solution was prepared. In analyzing samples in solution there is a large background to account for, however it was possible to

get a spectrum. Figure 12 compares the spectrum of $CaCl_2 \cdot 2H_2O$ in solution to a dry spectrum of the same salt. It is clear that there are differences in the position of the peaks but also in the relative intensities. In the crystal structure of $CaCl_2 \cdot 2H_2O$, the Ca^{2+} ion is coordinated with two waters and four chlorides.[13] In a 0.5M $CaCl_2 \cdot 2H_2O$ solution, calcium is expected to be Ca^{2+} surrounded by water ligands. A combination of Molecular Dynamics (MD) and Extended X-ray Absorption Fine Structure (EXAFS) spectra, indicate that aqueous Ca^{2+} is surrounded by an average of seven water ligands.[14] Given that a changing crystal field will influence the spectra, the spectrum of $CaCl_2 \cdot 2H_2O$ is expected to differ from the spectrum of Ca^{2+}. Ca^{2+}(aq) has seven neutral ligands whereas $CaCl_2 \cdot 2H_2O$ is coordinated by four chloride anions in its crystal structure. The anionic ligands in $CaCl_2 \cdot 2H_2O$ result in more electron density being donated to the metal, thereby strengthening the metal-ligand interaction. On the other hand, neutral water ligands will have a different influence with respect to electron sharing with the metal. Another difference between the two that will be reflected as a change in the spectra is the different coordination geometries. A change in the crystal field of calcium is noticeably reflected in the Ca 2p spectra.

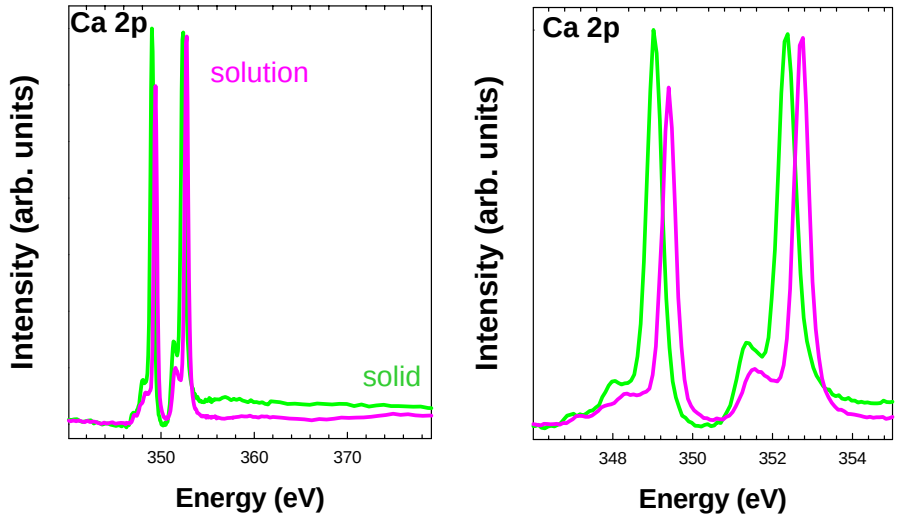

Figure 12 – Ca 2p spectra of calcium chloride dihydrate ($CaCl_2 \cdot 2H_2O$) in solution (purple) and solid phase (green) (STXM ALS).

Application

Now that reliable Ca 2p spectra have been established for a number of calcium compounds, it is possible to use them to assist analyzing a biofilm sample for its calcium components. A biofilm sample from natural river water collected from the South Saskatchewan River in Saskatoon, Saskatchewan was cultured using 1% methanol to stimulate growth. A STXM sample was prepared at McMaster University by freezing and cryomicrotoming. A region of the sample was analyzed using STXM (CLS, Dec. 06) to investigate both the calcium and oxygen energy regimes. Observation of the Ca 2p and O 1s edges helped in identifying and mapping both the organic and mineral portions of the sample.[15] Figure 13 shows the distribution maps of $CaCO_3$, protein and polysaccharide, produced by mapping the region based on their O 1s spectra.

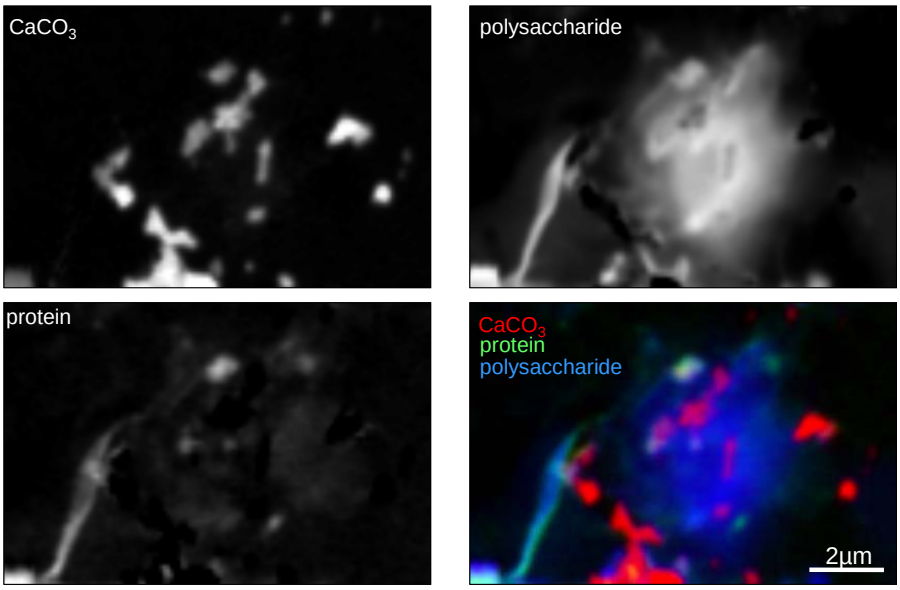

Figure 13 – River sample components $CaCO_3$, protein (indicating parts of cells), and biological polymers (composed of polysaccharides).

The $CaCO_3$ (coded red in the colour composite) is found in well formed sub-micron sized crystals. These crystals are too thick to give unsaturated Ca 2p spectra. However it is possible to obtain reliable chemical identification by examining thin regions around the edge of the crystals (Figure 14). This suggested the presence of both aragonite-like and calcite-like solids. In addition a third Ca 2p spectral signature was clearly identified in the polysaccharide portion surrounding the crystals. Accurate maps of the three calcium species were then derived by excluding all images in the two strong (thus absorption saturated) peaks in the energy ranges of 348.5-349.5eV and 352-353eV. By this means the influence of absorption saturation was minimized.

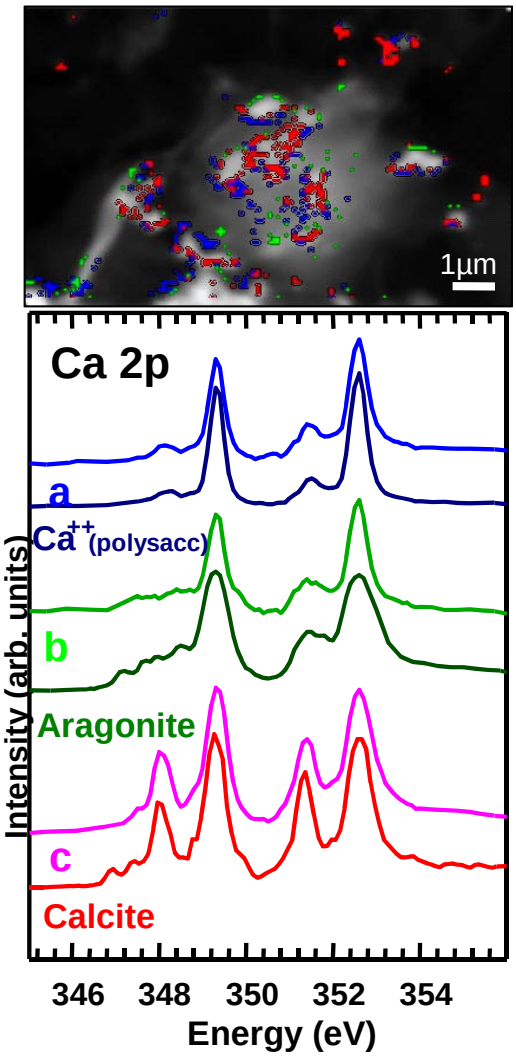

Figure 14 – a,b,c are Ca 2p spectra extracted from the corresponding coloured pixels in the image above. Reference spectra of Ca^{2+} (associated with polysaccharide), aragonite and calcite are shown for comparison.

A mask was generated and thin regions of the sample were found by selectively choosing sections near the edge of the thick crystals. Ca 2p reference spectra collected from pure dry samples were compared with the Ca 2p spectra extracted from the biofilm sample. In choosing the thinnest portions of the solid, it is assumed that the spectra are not being distorted by absorption saturation hence they can be compared with reference data. The spectra extracted in this fashion are a calcite like spectra (c), aragonite-like spectra (b) and Ca^{2+} spectra (a) associated with the polysaccharide portion of the sample. These

spectra suggest that the formation of calcite progresses from Ca^{2+} through the precursor aragonite before formation of the more thermodynamically stable calcite.[15] This is the first example to provide direct experimental evidence for a possible mechanism of calcite precipitation through an aragonite-like intermediate.

Future Work

In investigating organic and inorganic samples, STXM has strict sample requirements in terms of sample thickness in both dry and wet samples. The biofilm sample analyzed above was actually a dry sample. After seeing the success of the wet cell, the next step in the project is to investigate wet samples, which are closer to real life. One suggestion to increase the life of a sample in a wet cell is to assemble a flow system, in which there is a constant circulation of sample solution through the plenum area surrounding the Si_3N_4 windows. Another modification is using polyamide windows instead of silicon nitride ones, since polyamide is more robust. To increase confidence in the results of inner shell spectroscopy it would be meaningful to perform calculations to predict and better understand spectra. In calculating spectra for samples of calcite and aragonite, it may be possible to determine more specifically why the differences in the crystal structures (Figure 15) lead to such dramatic differences between the 4-peak structure of the Ca 2p spectrum of calcite and the 2-peak structure of aragonite.

By achieving a better understanding of biomineralization it is hoped that one day, a practical scheme can be developed in which calcite formation is artificially enhanced as a method of carbon sequestration. There are many steps between the current project and

this long-term goal such as the particular bacterial species capable of calcite formation, source of calcium for use by the bacteria, as well as the efficiency and cost of enhancing production in this manner. This research has shown that STXM is a powerful tool to study biomineralization. My contribution in this project was the development of a wet cell and derivation of reliable Ca 2p reference spectra to provide a solid foundation on which progress can be based. This research has advanced the methods and techniques presently being used and thereby contributed to use of STXM as a tool to understand biomineralization.

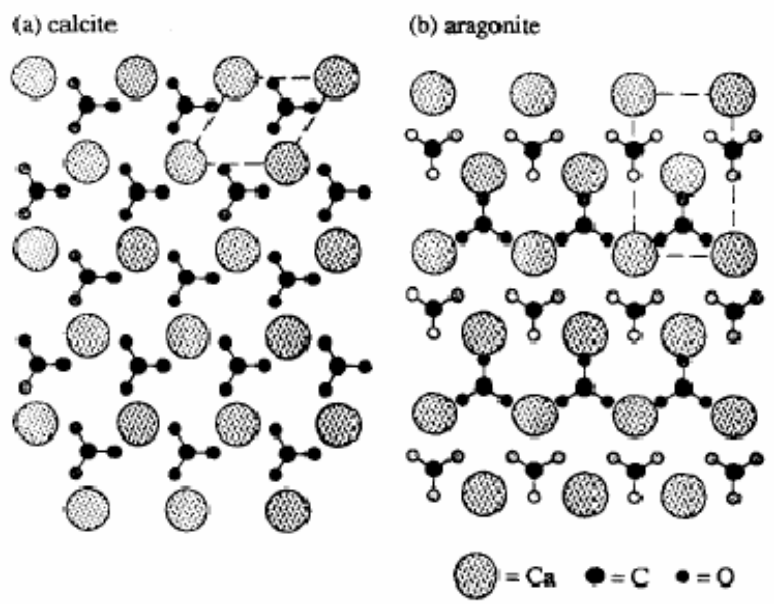

Figure 15 – Crystal structures of calcite and aragonite with unit cells outlines.[16]

Acknowledgements

This work is supported by NSERC, performed at CLS which is supported by NSERC, NRC, CIHR and the University of Saskatchewan. I thank the McMaster major facilities access fund for financial assistance. The author acknowledges the excellent sample preparation by Marcia Reid (Electron Microscopy in MUMC) and Michael Roberts of the McMaster University Science and Engineering Machine Shop for his work on the wet cell. Thank you to Martin Obst, Jay Dynes and Bonnie Leung as well as the entire

Hitchcock research group for their help and support. Thank you to my supervisor Adam Hitchcock, for the lessons.

References

1. Kouwenberg, L. et al. *Geology*, **33**(1), 33-36 (2005).
2. Ametistova, L.; Twidell, J.; Briden, J. *The Science of the total environment,* **289**(1-3), 213-23 (2002).
3. De Craen, M.; Swennen, R.; Keppens, E. M.; Macaulay, C. I.; Kiriakoulakis, K. *Journal of Sedimentary Research*, **69**(5), 1098-1106 (1999).
4. Klein, M.; Koren, N. *Limnologica*, **28**(3), 293-299 (1998).
5. Elder, F.R.; Gurewitsch, A.M.; Langmuir, R, V. *Phys. Rev.* **71** (11), 829-830 (1947).
6. Zhang, W. *Microwave and Optical Technology Letters.* **23** (2), 69-73 (1999).
7. Rightor, E.G.; Hitchcock, A.P.; Ade, H.; Leapman, R.D.; Urquhart, S.G.; Smith, A.P.; Mitchell, G.; Fischer, D.; Shin, H.J.; Warwick, T. *J. Phys. Chem. B* **101**, 1950-1960 (1997).
8. Stollberg, H.; Pokorny,M.; Hertz,H.M. *J. Microscopy* (2007)
9. Tröger, L.; Aravanitis, D.; Baberschke, K. *Phys. Rev. B.* **46**(6), 3283-3289 (1992).
10. Liu. D. et al. *Opt. Rev.* **13**(4), 235-238 (2006).
11. de Groot, F. *Cood. Chem. Rev.*, 1-33 (2004).
12. Himpsel, F.J.; Karlsson, U.O.; McLean, A.B.; Terminello, L.J. *Phsy. Rev. B* **43** (9), 6899-6907 (1991).
13.LeClaire, A.; Borel, M.M. *Acta Cryst.* **B33**, 1608-1610 (1977).
14. Jalilehvand, F. *J. Am. Chem. Soc., **123**(3)*, 431-444 (2001).
15. Obst, M. et al. $CaCO_3$ biomineralization in river biofilms. *CLS Annual Report,* (2006).
16. *Spectroscopy Letters*, **28**(6), 983-995, (1995).
17.Lawrence, J.R.; Swerhone, G.D.W.; Leppard, G.G.; Araki, T.; Zhang, X.; West, M.M.; Hitchcock, A.P. *Appl. Environ. Microbiol.* **69** (9), 5543-5554 (2003).